ADVANCED FUNCTIONAL MATERIALS
www.afm-journal.de

Bioengineered Gastrointestinal Tissues with Fibroblast-Induced Shapes

Linna Zhou, Carlos Ruiz-Puig, Brittany-Amber Jacobs, Xiaoyue Han, Richard Lisle, Hagan Bayley, and Xin Lu**

Bioengineered gastrointestinal (GI) tracts have potential applications in regenerative medicine and disease modeling. Methods for engineering tubular GI tracts containing natural extracellular matrix (ECM) are currently limited. Here, the fabrication of collagen tubes with designed shapes by using lipid bilayer supported droplet networks is reported. Droplets containing cells and collagen are arrayed in lipid-containing oil to form droplet networks, which undergo thermal gelation to provide continuous collagen tubes. A variety of tubular GI tissues are fabricated. For example, human intestinal organoids embedded in the collagen tubes migrate to the luminal surfaces and fuse to form a continuous epithelial layer, mimicking aspects of intestinal tissue structure. Fibroblasts embedded in the collagen induce a cell density dependent contraction of the tubes. Complex tubular structures are produced by patterning droplets containing different densities of fibroblasts. The fibroblast-containing collagen tubes are seeded with various epithelial cells at their luminal surfaces to form gastric and colonic tissues, which comprise monolayers or multilayers of epithelial cells and fibroblast-containing subepithelial layers. The engineered gastric tissues are susceptible to infection with *Helicobacter pylori*. The versatile technique allows the construction of tubular GI tracts containing ECM and layered structures, with broad potential applications in disease research and regenerative medicine.

1. Introduction

The gastrointestinal (GI) tract is essential for the intake of nutrients and digestion, drug absorption, and immune defense.[1] Functional disorders of the GI tract can result in gastrointestinal diseases, including gastric and peptic ulcer disease, and irritable bowel syndrome (IBS). In the UK, GI disorders account for around 10% of all clinical practice and IBS alone affects around 20% of the general population.[2] Despite their widespread occurrence, the majority of GI disorders are difficult to diagnose and manage. Moreover, severe GI diseases require surgical resection, and patients may subsequently require transplantation in the event of short bowel syndrome.[3] Bioengineered GI tracts are highly desirable for both disease modelling and tissue implantation.[4] Specifically, in vitro GI models allow simplified and well controlled conditions for the study of toxicology, drug absorption, and host–microbial interaction at lower cost compared to animal models.[5] Further, surgical resection of GI tracts produce complications and low quality of life, and bioengineered GI tracts have the potential to repair the function of lost tissues.[6]

GI tract bioengineering is particularly challenging because of its complex cellular composition and organization. To have broad application, a bioengineering strategy would fulfil certain criteria. From a biological standpoint, engineered GI tracts require multiple cell types arranged in a defined pattern, and must comprise biocompatible materials. From a technical perspective, the technology needs to have the flexibility to generate tubular structures of different sizes and shapes, and be simple to apply.

A common strategy for the bioengineering of GI tracts is to use scaffold materials in combination with tissue-specific cells or stem/progenitor cells. Efforts have focused on both the construction of tubular structures and the formation of epithelial layers, which are important for the absorption of nutrients and defense against pathogenic microbes.[1] Importantly, the nature of the chosen scaffold affects both the attachment and the fate of the seeded cells. Therefore, collagen, an extracellular matrix (ECM) protein, has frequently been added into nonbiocompatible scaffold materials, such as chitosan and silk, to support the seeded cells.[7–9] A collagen coating process is also required for scaffolds derived from synthetic polymers, for example, polyglycolic acid and poly-L-lactic acid.[10–12] These scaffold materials are mechanically stiffer than ECM and cells are unable to bind to them. Therefore, they are incompatible with the GI system.

Dr. L. Zhou, Dr. C. Ruiz-Puig, B.-A. Jacobs, Dr. X. Han, R. Lisle, Prof. X. Lu
Ludwig Institute for Cancer Research
Nuffield Department of Medicine
University of Oxford
Oxford OX3 7DQ, UK
E-mail: xin.lu@ludwig.ox.ac.uk
Dr. L. Zhou, Prof. H. Bayley
Department of Chemistry
University of Oxford
Oxford OX1 3TA, UK
E-mail: hagan.bayley@chem.ox.ac.uk
The ORCID identification number(s) for the author(s) of this article can be found under https://doi.org/10.1002/adfm.202007514.

© 2020 The Authors. Advanced Functional Materials published by Wiley-VCH GmbH. This is an open access article under the terms of the Creative Commons Attribution-NonCommercial License, which permits use, distribution and reproduction in any medium, provided the original work is properly cited and is not used for commercial purposes.

DOI: 10.1002/adfm.202007514

© 2020 The Authors. Advanced Functional Materials published by Wiley-VCH GmbH

Another strategy is to use decellularized tissue as a scaffold. This method preserves some of the native ECM proteins and the overall tissue structure, and allows recellularization with a patient's own cells to reduce immunogenicity.[13,14] However, the decellularized scaffolds require donor or animal tissues and are technically laborious to prepare. Nevertheless, bioengineered GI tracts, derived from both synthetic and decellularized scaffolding materials, have shown encouraging preclinical results in rodents.

The use of collagen without additional scaffold materials has the advantage of being fully biocompatible. Collagen is known to support cell proliferation, migration, and differentiation, and also to be remodeled by cells.[15,16] However, collagen derived hydrogels are generally soft and slow to gelate. These difficult mechanical properties prevent fabrication into defined structures. Collagen has been molded into micropatterns for the 3D culture of intestinal cells. However, the molded structures were small, not tubular, and required chemical crosslinking to increase the stiffness of the collagen for the molding process.[17] Polished glass molds have also been developed to support the fabrication of tubular vascular tissues.[18,19] However, the method lacks the potential for rapid production of collagen tubes with various sizes and complex shapes. A method developed by Sachs et al. fabricated collagen rings simply by adding collagen solution, seeded with mouse intestinal organoids, to the edges of the wells of 24-well plates.[20] The contraction of the collagen rings resulted in the alignment and fusion of the organoids at the center of the collagen rings to give macroscopic epithelial tubes. This straightforward approach generated centimeter-long intestinal tubes. However, the collagen rings were thin and irregular. Moreover, the intestinal tubes were embedded inside the collagen rings and not exposed for further manipulation, such as infection with a pathogen, which limits the potential applications of this technique.

Here, we report a simple, versatile means to construct tubular GI tracts from collagen without additional synthetic polymers or chemical modifications. We show that collagen tubes with different sizes and shapes can be constructed from lipid bilayer supported droplet networks arrayed in 3D printed molds. We demonstrate the generation of tubular GI tissues with both epithelial and subepithelial structures, the controllable contraction of the collagen tubes by fibroblast density to produce complex shapes, and infection of the engineered gastric tissues.

2. Results

2.1. Engineered Collagen Tubes from Droplet Networks

Previously, we reported the production of 3D droplet networks bonded together by adhesive droplet-interface lipid bilayers.[21,22] Different droplet contents have been explored to produce droplet network derived synthetic and living tissues, with overall dimensions of hundreds of micrometers to millimeters.[22–26] Here, we report a modified droplet-based method that uses molds to support large and hollow droplet networks for the production of collagen tubes with centimeter dimensions. Droplets, containing cells and collagen solution, generated in lipid-containing oil, spontaneously acquired a monolayer of lipids (**Figure 1**a). When droplets were in contact, lipid bilayers were formed at their interfaces. Partial gelation of the collagen occurred when the droplets were incubated at room temperature (RT) for 10 min. Dilution of the lipids and further incubation at 37 °C led to the breakdown of the droplet-interface bilayers, and the collagen gelated further to form a continuous structure. After gelation at 37 °C for 20 min, the templated shapes were transferred into cell culture medium.

To fabricate collagen tubes, we generated a hundred to over a thousand droplets, each of ≈2 μL, to form droplet networks inside supporting molds of various sizes, 0.5–10 cm in length (Figure 1b and Figure S1, Supporting information). The molds were 3D printed based on design by using the polymers acrylonitrile butadiene styrene (Figure 1c). After 10 min at RT, lipid dilution and then 20–60 min at 37 °C (see the Experimental Section), continuous tubular structures were formed, which were removed from the molds to give free standing tubular structures with defined dimensions (Figure 1c,d).

2.2. Engineered Intestinal Tissues from Fused Organoids

Intestinal organoids are self-organized, microscopic structures that recapitulate the signaling and architecture relevant to the natural gut epithelium. Organoids are widely used for studying intestinal epithelium development, stem cell biology, and disease.[27] We advanced the method of Sachs et al. by using droplet network assembly and molds, to generate human intestinal tubes with defined structures and exposed lumens. Human duodenum organoids (HDOs), derived from patients, were embedded in 0.5 cm long collagen tubes (**Figure 2**a). Interestingly, with our method, the organoids migrated toward the luminal surface of the collagen tube, instead of the center of the collagen wall as reported by Sachs et al. (Figure 2b,c and Figure S2, Supporting Information). As observed by Sachs et al., fusion of the organoids occurred in the collagen rings after around 3 days of culture (Figure 2d). Further, we also observed contraction of the collagen tubes (Figure 2c and Figure S3, Supporting Information), which brought the organoids into close proximity and induce their fusion. Consistent with the data from Sachs et al., organoid migration and fusion were not observed when the HDOs were embedded in Matrigel-derived tubes (Figure S4, Supporting Information), indicating the importance of the contractility of the collagen.

Immunofluorescence staining of sectioned tubes showed an epithelial layer as a continuous monolayer at the luminal surface (Figure 2d). Like intact HDOs, the epithelial layer expressed the cell–cell junction protein E-cadherin, the intestinal marker villin and markers of other main intestinal cell types (Figure S5, Supporting Information). Therefore, the engineered intestinal tissues have a defined tubular shape and an exposed intestinal epithelial layer at the luminal surface, which resemble aspects of human intestinal structures.

© 2020 The Authors. Advanced Functional Materials published by Wiley-VCH GmbH

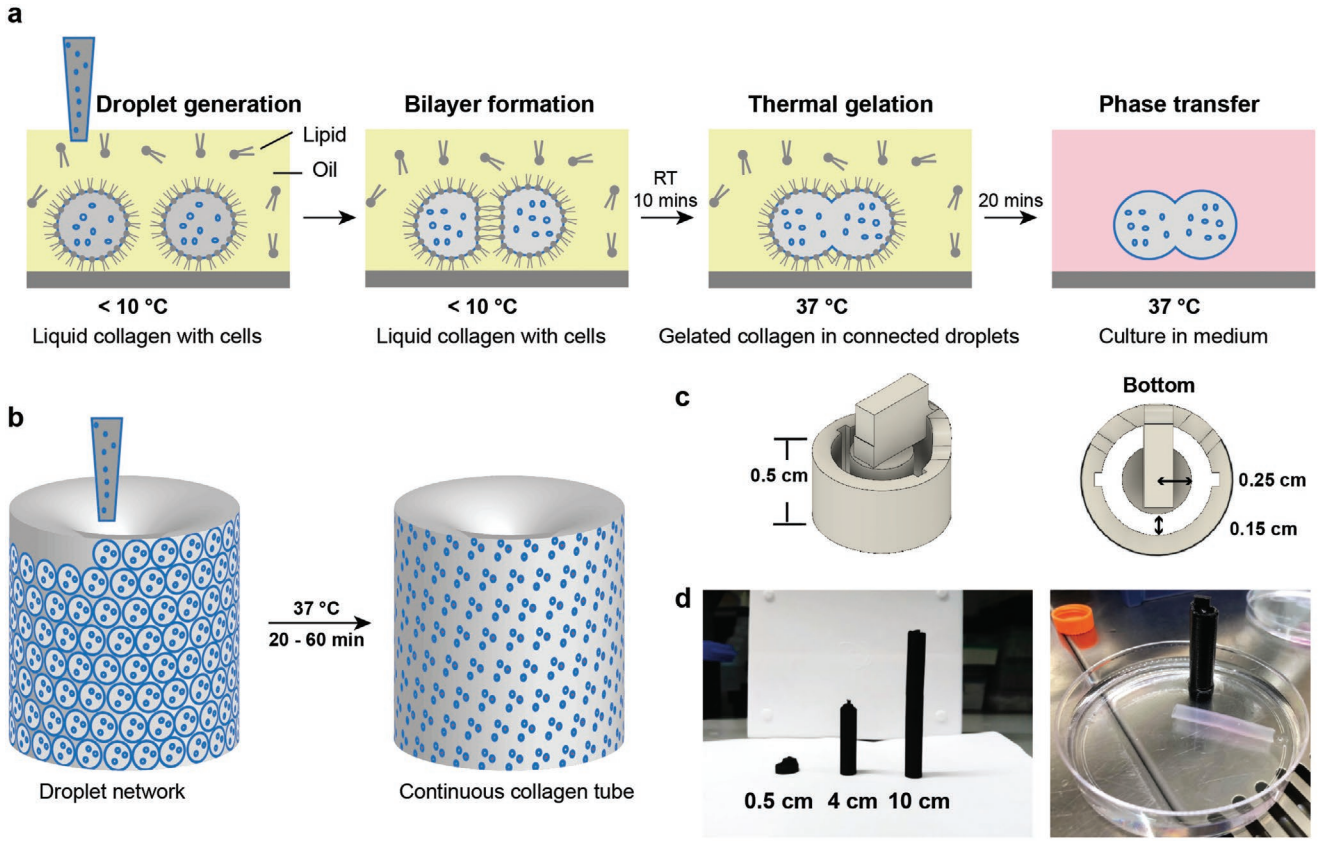

Figure 1. Engineered collagen tubes from droplet networks. a) Schematic showing the adhesion of droplets containing collagen and cells. Left to right: water-in-oil droplets spontaneously acquire a monolayer of lipids in lipid-containing oil. Upon contact, droplets form a lipid bilayer at the droplet interface. Incubation of the droplets at room temperature (RT) for 10 min allows partial gelation of the collagen. Dilution of the lipid and an increase of the temperature to 37 °C leads to the breakdown of the lipid bilayer and fusion of the droplets. After gelation, the structure can be transferred into culture medium. b) Schematic for the fabrication of a collagen tube from a droplet network. Droplets were arrayed into a tube-shaped network (supported by a mold, as in (c) and (d)). The incubation steps described in (a) produced a continuous tubular structure containing collagen and cells. c) An example of a 3D printed mold, which supported the generation of collagen tubes with an internal diameter of 0.25 cm, a wall thickness of 0.15 cm, and a length of 0.5 cm. d) Left: 3D printed molds of different lengths, 0.5, 4, and 10 cm. Right: a tube (4 cm) generated from droplets containing collagen at 1.6 mg mL^{-1}.

2.3. Fibroblast-Induced Contraction for the Production of Complex Tubular Shapes

In GI tracts, fibroblasts underlie the epithelial layer and contribute to epithelial cell homeostasis, inflammation, and wound healing.[28–30] In previous attempts to recapitulate subepithelial fibroblast involvement in bioengineered esophagus or intestine, epithelial cells have been seeded on top of fibroblasts embedded in collagen sheets or tubular scaffolds, derived from polyglycolic acid or silk.[8,31,32]

Fibroblasts are able to synthesize ECM and induce contraction in collagen gels, and the latter has been used to study wound healing for decades.[33] We constructed 0.5 cm long collagen tubes containing fibroblasts at different cell densities: 0, 50, 250, and 500×10^3 mL^{-1} (**Figure 3**a). In the absence of fibroblasts, no contraction was observed over 48 h. By contrast, the collagen tubes contracted over time when fibroblasts were present, and both the rate and extent of the contraction increased with fibroblast density (Figure 3a). With 500×10^3 mL^{-1} fibroblasts, the outer diameter of the tubes had decreased by over 80% after 48 h. We also demonstrated the contraction of a 4 cm long tube (Video S1, Supporting Information). Immunofluorescence staining confirmed the presence of collagen I, which was used to form the tubes (Figure 3b).

To construct complex tubular structures with segments of different diameter, we patterned droplet networks by using droplets containing fibroblasts at different densities to form the various segments (Figure 3c). Immediately after formation, the patterned collagen tubes were of uniform internal diameter. However, after 48 h of culture, the segments with higher fibroblast density had narrowed, compared to those of lower fibroblast density, i.e., the internal diameter of the tubes could be tuned by adjusting the fibroblast density (Figure 3a). Two shapes, Shape 1 and Shape 2, were produced (Figure 3d). Shape 1 started from a 4 cm long tube and contained five segments which resulted a stomach-like structure (Figure S6, Supporting Information and the Experimental Section). Shape 2 started from a 10 cm long tube and contained nine segments. These examples demonstrate a simple method, combining the droplet network technique and fibroblast-induced contraction, to produce complex tubular structures.

© 2020 The Authors. Advanced Functional Materials published by Wiley-VCH GmbH

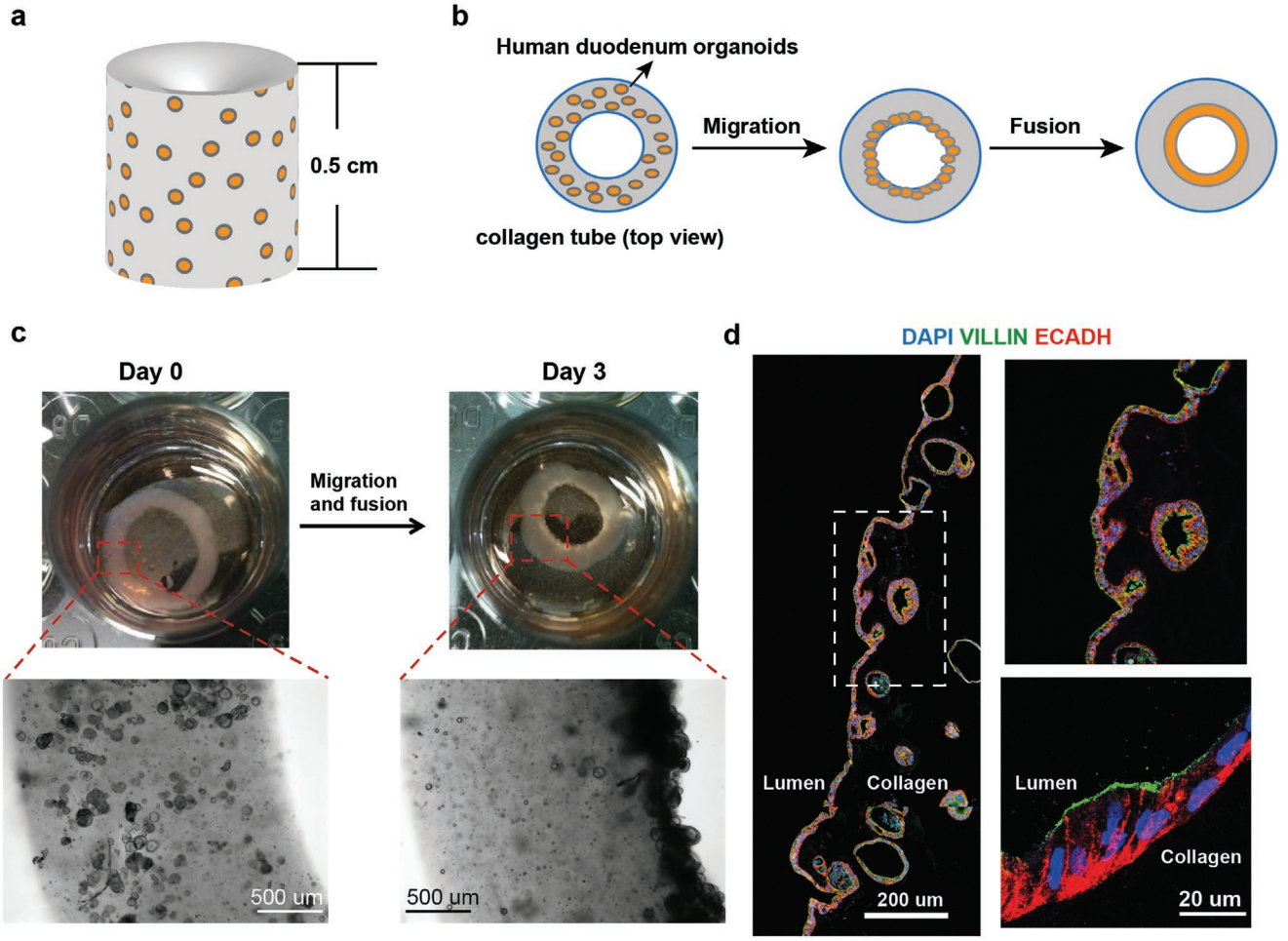

Figure 2. Human intestinal tissues constructed from fused intestinal organoids. a) Schematic of an intestinal tissue containing human duodenum organoids (HDOs, orange circles). b) Schematic of the migration and fusion of HDOs in collagen tubes. c) Images of 0.5 cm collagen tubes containing HDOs at day 0 and day 3 postfabrication. The organoids moved to the luminal surface of the tube where they fused to form a continuous epithelial layer. The red boxes indicate the areas of the higher magnification images (below). d) Immunofluorescence demonstrates the fused, continuous epithelial layer at the luminal surface of the tube. The epithelial cells expressed the cell–cell junction protein E-cadherin (ECADH) and the intestinal marker villin. The dashed box indicates the area of higher magnification (top right). The image at the bottom right shows the epithelial layer at high magnification (64×).

2.4. Engineered Gastrointestinal Tissues Using Fibroblast-Containing Collagen Tubes

Next, we tested whether different types of epithelial cells could be seeded onto the luminal surface of the fibroblast-containing collagen. First, we constructed gastric tissues by using Shape 1 (see above) to mimic the stomach. After 48 h in culture, the fibroblast-containing tubes were sufficiently robust for further manipulation. The tubes were sealed at one end and then dissociated gastric adenocarcinoma epithelial cells (AGS cells) were injected to the lumen, followed by sealing of the other end of the tube (**Figure 4**a). After 24 h, unattached AGS cells were washed out with fresh medium. The engineered gastric tissues were then fixed and sectioned. Hematoxylin and eosin (H&E) staining revealed the formation of a monolayer of AGS cells around the luminal surface (Figure 4b), while collagen I immunostaining showed the collagen used for the tube construction (Figure 4c). Staining for the epithelial markers cytokeratin 8 and E-cadherin further confirmed the monolayer structure and its epithelial identity.

To demonstrate the versatility of the technique, we also constructed colonic tissues by seeding human colon carcinoma epithelial cells (Caco-2 cells) into collagen tubes containing 500×10^3 mL^{-1} fibroblasts. Interestingly, H&E staining showed that the epithelial layer consisted of a multilayer of Caco-2 cells (Figure 4d), consistent with the behavior of these cells in confluent 2D cultures.[34,35] 4′,6-Diamidino-2-phenylindole (DAPI) staining and collagen I immunostaining confirmed the multilayer epithelial structure and its location at the luminal surface of the collagen tube (Figure 4e). The epithelial cells also expressed the epithelial marker cytokeratin 8 and the cell–cell junction marker E-cadherin.

To show a potential application of our bioengineered GI tracts, we conducted infection experiments with *H. pylori*, which can cause gastritis, peptic ulcers and gastric cancer.[36] *H. pylori* suspended in AGS cell culture medium were added to

© 2020 The Authors. Advanced Functional Materials published by Wiley-VCH GmbH

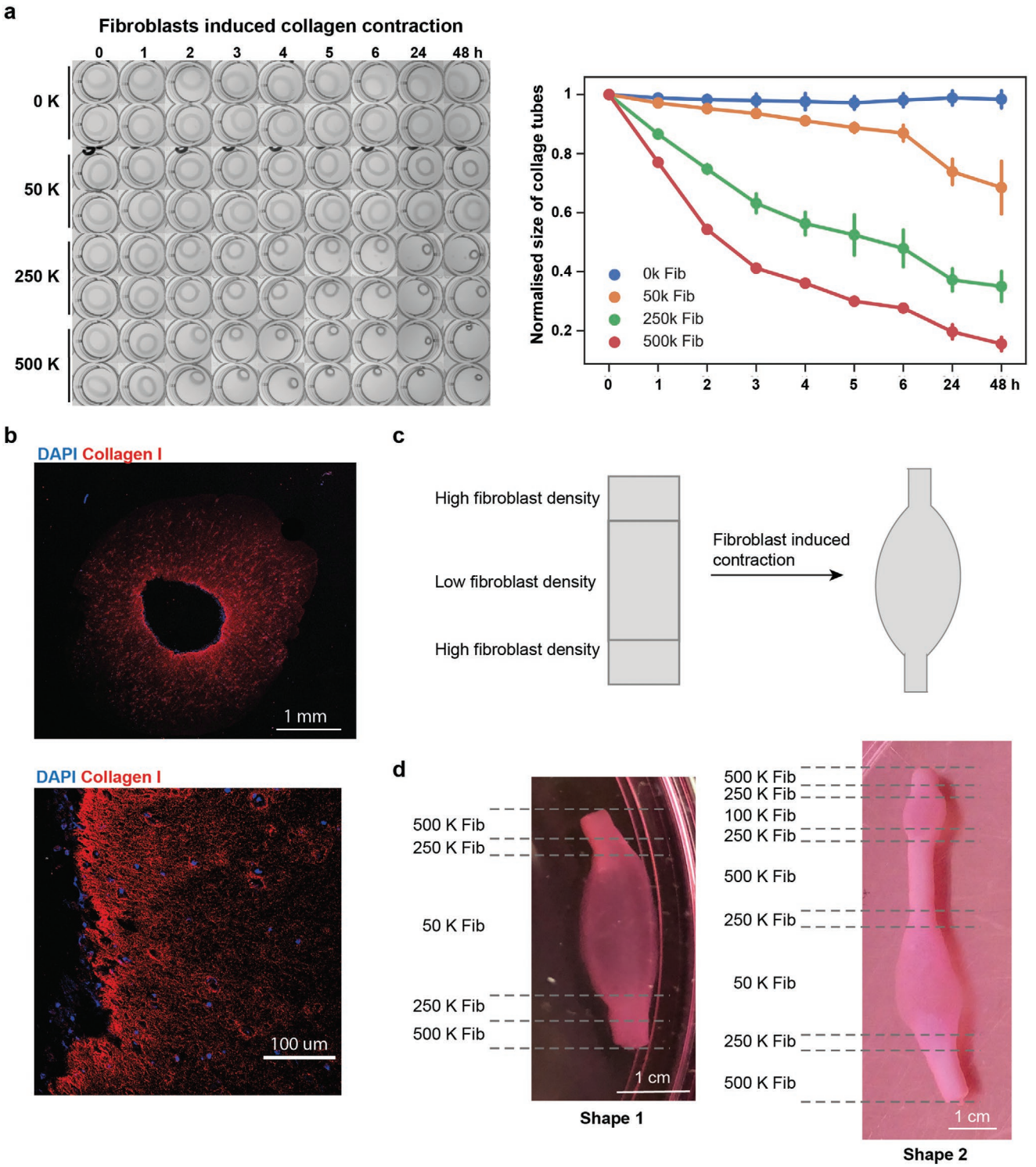

Figure 3. Fibroblast-induced contraction produces various tubular shapes. a) Fibroblast-induced contraction was cell density dependent. Left: contraction of the collagen tubes over 48 h at various fibroblast densities: 0, 50, 250, 500 × 10^3 mL^{-1}. Right: quantification of the change of the outer diameter of the collagen tubes over 48 h. The sizes of the tubes were normalized to 1.0 at $t = 0$. $n = 3$, for all conditions. Fib stands for fibroblasts. b) Immunofluorescence of a collagen tube containing 500 × 10^3 mL^{-1} fibroblasts. Top: cross-section; bottom: higher magnification image. The Collagen I and DAPI staining reflected the collagen and cell content. c) Strategy used for the generation of shaped collagen tubes by patterning with droplets containing fibroblasts at various densities. The higher the fibroblast density used, the greater the contraction induced in the collagen tubes. d) Images of two shaped collagen tubes. Left: Shape 1 with 5 segments containing 500 × 10^3, 250 × 10^3, 50 × 10^3, 250 × 10^3 and 500 × 10^3 fibroblasts mL^{-1} (top to bottom). Right: Shape 2 with 9 segments containing 500 × 10^3, 250 × 10^3, 100 × 10^3, 250 × 10^3, 500 × 10^3, 250 × 10^3, 50 × 10^3, 250 × 10^3, and 500 × 10^3 fibroblasts mL^{-1} (top to bottom).

© 2020 The Authors. Advanced Functional Materials published by Wiley-VCH GmbH

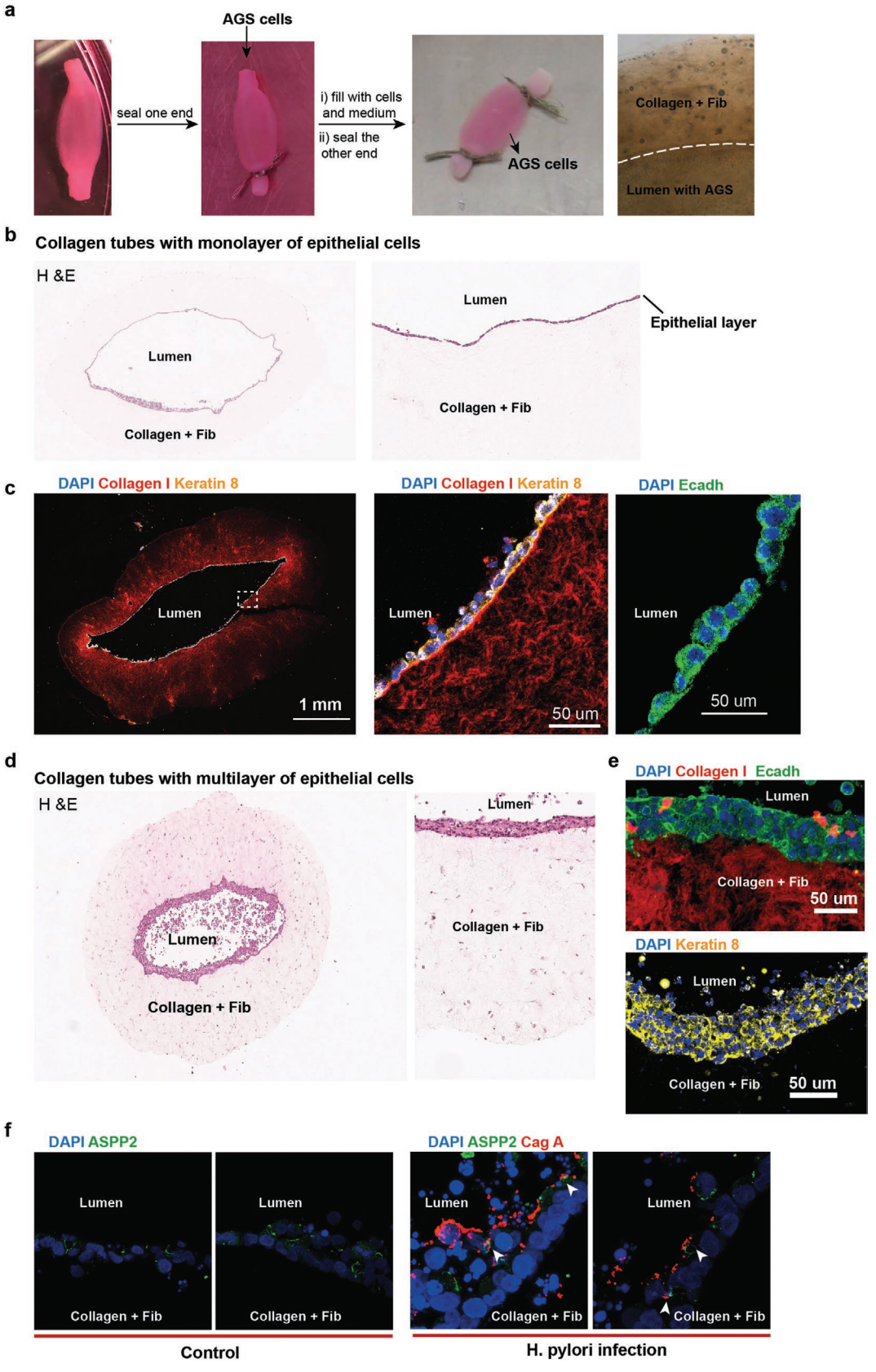

© 2020 The Authors. Advanced Functional Materials published by Wiley-VCH GmbH

the lumen of the gastric tubes (Figure 4a–c). After 6 h, the tubes were washed and examined by immunofluorescence. Staining for cytotoxin-associated gene A (CagA), which is expressed by *H. pylori*, confirmed that the pathogen was able to infect the epithelial cells in the gastric tubes (Figure 4f). Further, the colocalization of CagA and the apoptosis-stimulating protein of p53 2 (ASPP2) indicated the recruitment of ASPP2 by CagA during infection.[37]

3. Discussion

Hydrogels derived from ECM proteins, such as collagen and Matrigel, are soft and slow to attain full gelation from the liquid state. Therefore, it is difficult to fabricate these hydrogels into defined structures, due to their tendency to deform. Previous molding methods for the construction of collagen tubes relied on the use of polished glass molds,[18,19] which is a less flexible approach for the fabrication of tubes of various sizes and shapes compared to the use of 3D-printed plastic molds. However, our attempts to generate collagen tubes by directly adding collagen to the molds led to difficulties: the collagen gel easily stuck to the plastic molds and the constructed tubes broke easily during removal from the molds. Further, cells and organoids sank to the bottom of the constructs due to gravity. The use of oil and lipids in our method stopped the collagen gel sticking to the molds, and the compartmentalization with droplets prevented the gravity-induced sinking of cells and organoids during the construction process. Furthermore, patterns could be generated within the droplet networks. By patterning segments of the tubes with different fibroblast densities, we produced shapes of more complexity than simple tubes.

Moreover, the method of Sachs et al. generated flat collagen rings with limited control over the thickness of the rings and their general shape. Here, we have developed a method to generate structurally defined collagen tubes with an exposed lumen, without the need for the addition of synthetic polymers or chemical crosslinking. The technique allowed us to use low collagen concentrations, 1.0 and 1.6 mg mL^{-1} (the Experimental Section), but higher collagen concentrations might be employed. The use of collagen at different concentrations is important for the production of GI tissues of varying mechanical stiffness.

Yet more varied collagen tubes might be generated by varying the design of the 3D printed molds. For example, molds with branched shapes could be used to generate branched tubes for the formation of vascular tissues.

To demonstrate the versatility of the technique, we constructed various tubular GI tissues, including intestinal, gastric and colonic tissues. The engineered tissues contained epithelial layers at their luminal surfaces and subepithelial fibroblasts embedded in the collagen wall, mimicking the layered structure of GI tracts. Therefore, we provide a simple, biocompatible technique to build layered tubular GI tissues. Other subepithelial types, such as muscle cells, immune cells and enteric neurons, might be also embedded in the collagen, to study their interaction with the epithelial cells under both normal and disease conditions. Further, multiple subepithelial layers could be generated by combining the current technique with the automated 3D droplet printing technique, previously developed.[21,22] This would allow us to create multiple subepithelial layers, each containing different cell types, in the collagen wall of the tubes. These multiple layered GI tissues would closely resemble the complex cellular architecture of GI tissues, and might be implanted to treat short bowel syndrome or make humanized models in rodents. Finally, we also demonstrated that a pathogen can be added to the lumen to infect the bioengineered GI tracts. In the future, luminal flow could be introduced to the bioengineered GI tracts to recapitulate physiological conditions and study the effects of pathogens and toxins.

4. Experimental Section

3D Printed Supporting Molds: The supporting molds were computer designed using Fusion 360 software. The designs were then rendered for printing using Cura software. The printing was performed by an Ultimaker 2+ 3D printer using polymer acrylonitrile butadiene styrene.

Fabrication of Collagen Tubes: Collagen type I (Corning/354249) solution was diluted and neutralized to pH 7.3 according to manufacturer's instructions with cell culture medium, with a final concentration of 1 or 1.6 mg mL^{-1}. The prepared collagen was kept on ice prior to use.

To construct the collagen tubes from arrayed droplet networks, sterilized molds were submerged in an oil bath, which consisted of 4 mg mL^{-1} 1,2-diphytanoyl-*sn*-glycero-3-phosphocholine (DPhPC, Avanti, 850356) in a mixture of undecane and silicone oil AR20 (both from Sigma Aldrich; v:v, 1:4). Collagen droplets, ≈2 µL in size, were pipetted into the molds to form droplet networks. The networks were left to settle for 10 min. Half of the lipid containing oil was then removed and replaced with undecane to dilute the lipid concentration and ensure the subsequent breakdown of the lipid bilayers. The collagen tubes were allowed to gelate at 37 °C for 20, 40, or 60 min for 0.5, 4 or 10 cm long collagen tubes respectively. The oil was subsequently removed

Figure 4. Engineered tubular gastrointestinal tissues with epithelium and subepithelium structures. a) Seeding epithelial cells into the lumen of fibroblast-containing collagen tubes. Collagen tubes of Shape 1 (Figure 3d) were used to mimic the stomach. The tube was first sealed at one end. Then dissociated gastric adenocarcinoma epithelial cells (AGS) in culture medium were injected into the lumen of the tube through the other end, which was subsequently sealed. After 24 h, AGS cells attached to the lumen of the tube and formed a monolayer of epithelial cells. The dotted line in the brightfield image (right) indicates the interface between the collagen wall and the lumen of the tube. b) H&E staining shows the monolayer of AGS cells around the lumen. c) Immunofluorescence confirmed the expression of the epithelial markers cytokeratin 8 and E-cadherin in the monolayer. The dashed box indicates the area of higher magnification (middle image). d,e) Engineered colonic tissues with a multilayer of epithelial cells. The fabrication process was similar to that in (a) but the collagen tubes contained fibroblasts (500×10^3 mL^{-1}) and colorectal adenocarcinoma cells (Caco-2) as the epithelial cells. d) H&E staining shows the multilayer of Caco-2 cells at the luminal surface of the tissue. e) Immunofluorescence confirmed a multilayer epithelial structure, which also expressed the epithelial marker cytokeratin 8 and the cell–cell junction protein E-cadherin. Collagen I staining confirmed the structure of the tubes. f) *H. pylori* were injected into the lumen of the bioengineered gastric tubes to infect epithelial cells. The tubes were infected for 6 h before being processed. Immunofluorescence showed the co-localization of CagA (*H. pylori* marker) and ASPP2 (a junctional protein recruited by CagA during infection) next to the epithelial cells (white arrows).

© 2020 The Authors. Advanced Functional Materials published by Wiley-VCH GmbH

and 2 washes with 1 × PBS were performed. Using sterile forceps, the supporting molds were carefully removed and a further two washes with PBS were conducted to give the self-supporting collagen tubes.

Duodenum Organoid Derivation and Maintenance: Duodenum biopsies were collected from outpatients during endoscopy at the John Radcliffe Hospital, Oxford, with written informed consent (through the Oxford Gastrointestinal Illness Biobank, authorised by Yorkshire & The Humber - Sheffield Research Ethics Committee: 16/YH/0247; laboratory research using the samples authorised by South Central - Oxford C Research Ethics Committee: 09/H0606/78). Healthy biopsies from Barrett's Esophagus patients were collected in Advanced DMEM/F12 supplemented with 1% 2×10^{-3} M L-glutamine, 2 µL mL^{-1} 1 M (4-(2-hydroxyethyl)-1-piperazineethanesulfonic acid (HEPES, pH 7.4) and 200 U mL^{-1} penicillin/streptomycin and kept on ice prior to processing.

To derive human duodenum organoids, the protocols of Sato et al. and O' Rourke et al. were followed.[38,39] The tissue was cut into small (≈5 mm) pieces and repeatedly washed with ice-cold 1 × PBS until the supernatant was clear. The tissue fragments were then incubated with cold 5×10^{-3} M ethylenediaminetetraacetic acid (EDTA)–PBS and placed on a roller at 4 °C for 15 min. To produce further dissociation, the tissue fragments were washed twice with ice-cold PBS and incubated in TripLE (ThermoFisher Scientific, 12605010) at 37 °C for 30 min. Following a further two washes with ice-cold PBS, the sedimented tissue fragments were vigorously resuspended in ice-cold PBS and allowed to settle under gravity. The supernatant, now enriched with cells released from the tissue fragments, was collected, passed through a 35 µm cell strainer and centrifuged at 200 × *g* for 5 min. The pellets were then embedded in Matrigel (Corning, 354230) and seeded in 24-well plates (≈30 µL of Matrigel/well). The Matrigel was allowed to gelate at 37 °C for 5 min and 500 µL of human organoid medium (Table S1, Supporting Information) was then overlaid and replaced every 2 days. To prevent anoikis, Rho-associated protein kinase (ROCK) inhibitor (Y-27632) and GSK-3 inhibitor (CHIR99021) were added to the medium for the first two days after derivation. Organoids were maintained at 37 °C in an atmosphere of 5% CO_2 and 95% humidity.

Organoids were passaged every 7–10 days at a ratio of 1:4 as follows. Using ice-cold PBS, the organoids were retrieved from the Matrigel and briefly microcentrifuged. To aid organoid dissociation, the pellet was vigorously resuspended in TripLE and incubated at RT for 5 min. The organoid fragments were then briefly microcentrifuged, embedded in Matrigel and seeded in 24-well plates (≈30 µL of Matrigel/well). The Matrigel was allowed to gelate at 37 °C for 5 min and 500 µL of human organoid medium was then overlaid and replaced every 2 days.

Human Organoid Conditioned Medium: HEK293T Rspo1-Fc cells, HEK293T Nog-Fc cells and L Wnt3A cells were used to generate R-Spondin-, Noggin-, and Wnt3A conditioned medium, respectively. Cells were maintained in the appropriate specified media (Table S2, Supporting Information) at 37 °C in an atmosphere of 5% CO_2 and 95% humidity.

To generate the conditioned medium, the stably transfected cells were initially grown in the relevant selectable medium (Table S2, Supporting Information) and then expanded considerably in the relevant nonselectable medium in order to produce sufficient quantities of conditioned medium. Cells were cultured for one week after which the medium was collected, sterile filtered (0.45 µm) and stored at −80 °C prior to use.

A HEK293T Wnt3A luciferase reporter cell line was used to test the quality of the R-Spondin and Wnt3A conditioned medium. Freshly made conditioned medium was tested against previously made batches and was only used for organoid culture if the same or better quality (detected as an increased luciferase reading and therefore Wnt3A promoter activity) was observed. In order to test the quality of the Noggin conditioned medium, organoids were cultured in human organoid medium containing the newly made Noggin conditioned medium and the growth monitored for 7–10 days. If the organoids began to die or grow at a slower rate, the conditioned medium batch was discarded.

Cell Culture of AGS, Caco-2, and Fibroblast Cells: The human stomach adenocarcinoma cell line, AGS (CRL-1739), and the human colorectal adenocarcinoma cell line, Caco-2 (HTB-37), were maintained in complete RPMI 1640 medium (Supporting Information) and the human fetal fibroblast cell line, HFF-1, was maintained in complete DMEM. Cells were cultured at 37 °C in an atmosphere of 5% CO_2 and 95% humidity.

Construction of Intestinal Tubes with HDOs: Harvested HDOs were washed with ice-cold PBS three times before being resuspended in the prepared 1 mg mL^{-1} collagen. HDOs from each confluent well of a 24-well plate were mixed with 200 µL collagen solution and 160 µL of the mixture was used to construct one 0.5 cm long collagen tube. The collagen tubes were incubated at 37 °C for 20 min and the construction process described above in the "Fabrication of collagen tubes" was subsequently followed. The constructed intestinal tubes were cultured in 600 µL of human organoid medium in a 24-well plate and the medium was replaced with fresh medium every second day.

Construction of Fibroblasts Containing Collagen Tubes: In general, harvested fibroblasts were resuspended in 1.6 mg mL^{-1} collagen to give the desired fibroblast densities. The construction process described in the "Fabrication of collagen tubes" was followed. For collagen tubes patterned with segments containing different fibroblast densities, an extra 5 min of incubation at RT were performed between the construction of different segments to allow sufficient time for the droplets to settle before the addition of droplets with a different fibroblast density. The 0.5, 4, and 10 cm long fibroblast-containing collagen tubes were incubated at 37 °C for 20, 40, and 60 min respectively.

To construct complex shape 1, a high fibroblast density, 500×10^3 mL^{-1}, was used for the narrow segments at the two ends of the collagen tube. Whereas a lower fibroblast density, 50×10^3 mL^{-1}, was used for the wider segment at the middle of the tube. A medium fibroblast density, 250×10^3 mL^{-1}, was used to smooth the transition between the narrow and wide segments. Similarly, a longer tube, complex shape 2, with nine segments was constructed to give a more complex structure. By using two low fibroblast densities, 100×10^3 and 50×10^3 mL^{-1}.

Seeding Epithelial Cells into Fibroblast-Containing Collagen Tubes: To seed epithelial cells to the luminal surface of the fibroblast-containing collagen tubes, one end of the tube was securely sealed with a sterile string. Then 1×10^6 AGS or Caco-2 cells suspended in 100 µL complete RPMI 1640 medium were introduced into the vertically held tube through the open end, which was subsequently also sealed. The tubes were placed in a 10 cm cell culture dish containing 10 mL of fibroblast medium and incubated at 37 °C in an atmosphere of 5% CO_2 and 95% humidity. To prevent an uneven distribution of cells, the tube was turned over after 3 h. After 24 h, one end of the tube was reopened and the inner surfaced rinsed with the appropriate medium before processing.

Helicobacter pylori Infection of Engineered Tubular Gastric Tissues: *H. pylori* (G27 strain) was cultured as previously described.[40] In order to infect AGS cells lining the luminal surface of the gastric tissues, the open end of a tube was filled with 1×10^9 *H. pylori* bacterium suspended in 100 µL of AGS medium without antibiotics. The open end was then resealed. The tubes were placed in a 10 cm cell culture dish containing 10 mL of fibroblast medium (without antibiotics) and incubated for 7 h at 37 °C in an atmosphere of 5% CO_2 and 95% humidity. After the incubation, the luminal surface of the tubes were thoroughly rinsed, and the tubes were prepared for processing.

Sample Processing: To prepare samples for staining, the collagen tubes were washed twice with PBS and fixed in 4% paraformaldehyde at 4 °C overnight. Samples were then processed in an automated tissue processor (ThermoFisher Scientific/Excelsior AS) to embed them in paraffin wax. The 0.5 cm-long tubes were embedded in HistoGel (ThermoFisher Scientific/HG-4000) prior to tissue processing and tubes longer than 0.5 cm were cut longitudinally prior to paraffin embedding and each section was individually processed. A microtome was used to cut 0.4 µm sections, which were mounted onto glass slides and dried at 37 °C. Before immunostaining, slides were incubated at 60 °C for 1 h and then processed accordingly to remove the paraffin wax. Further dehydration of the fixed samples was achieved by submerging them in Histoclear (2 × 5 min), 100% ethanol (1 × 1 min), 90% ethanol (1 × 1 min), and 70% ethanol (1 × 4 min) consecutively.

Immunofluorescence Staining: After processing, samples were boiled in 1× Tris–EDTA buffer (10×10^{-3} M Tris Base, 1×10^{-3} M EDTA, 0.05% Tween 20, pH 8.0) for 10 min and placed in a humidifying chamber. Antigen retrieval was performed according to the manufacturers' instructions. Samples were washed twice, permeabilized in 0.1% Triton-X for 15 min and blocked using Image-iT Fx Signal Enhancer (ThermoFisher Scientific/

© 2020 The Authors. Advanced Functional Materials published by Wiley-VCH GmbH

I36933) for 1 h. Samples were incubated in primary antibody (Table S3, Supporting Information) diluted in background reducing antibody diluent (Agilent Dako/S3022) at 4 °C overnight. Samples were then washed in PBS (3 × 10 min) and incubated in the appropriate secondary antibody diluted in antibody diluent (Agilent Dako/S0809) for 2 h in the dark. Finally, samples were washed 3 times with PBS and mounted using 200 µL of Prolong Gold Antifade mountant (ThermoFisher Scientific/P36930). The immunostained samples were imaged on a Zeiss 710MP confocal microscope.

Hematoxylin and Eosin Staining: For hematoxylin and eosin staining, processed samples were submerged consecutively in hematoxylin (1 × 5 min), H_2O (1×2 min), acidic alcohol (1×5 s), H_2O (1×2 min), Scott's Water (1 × 30 s), H_2O (1 × 2 min), eosin (1 × 5 min), H_2O (1 × 1 min), 70% ethanol (1 × 30 s), 90% ethanol (1 × 30 s), 100% ethanol (1 × 1 min), 100% ethanol (1 × 2 min), and histoclear (2 × 5 min). Slides were then mounted using VectaMount Permanent Mounting Medium (Vector Laboratories/H-5000) and imaged using a Hamamatsu Automated Slide Scanner. Analysis was performed using NDP.view2.

Time-Lapse Microscopy for Fibroblast Induced Contraction: Immediately after construction, time-lapse images of the fibroblast-containing collagen tubes were acquired using a Nikon TE 2000-E inverted microscope (Photometrics Prime camera) using a 2× objective. The tubes were maintained at 37 °C in an atmosphere of 5% CO_2 and images were acquired every hour for 48 h. Image analysis was performed using the MetaMorph software (Molecular Devices, LLC.) and processed into videos using Fiji ImageJ.

Supporting Information

Supporting Information is available from the Wiley Online Library or from the author.

Acknowledgements

The authors appreciate Mary Muers (Ludwig Institute for Cancer Research, Oxford) for assisting with manuscript preparation. The research was supported by the National Institute for Health Research (NIHR) Oxford Biomedical Research Centre (BRC), and also a European Research Council Advanced grant (SYNTISU) to H.B. L.Z., C.R.P., B.-A.J., X.H., R.L. and X.L. were supported by the Ludwig Institute for Cancer Research. The views expressed are those of the authors and not necessarily those of the NHS, the NIHR or the Department of Health. B.-A.J. was also supported by the Clarendon Fund and an Oxford Radcliffe Scholarship. The affiliations were updated to include the highest academic title for X. H. on February 3, 2021 after initial online publication.

Conflict of Interest

The authors declare no conflict of interest.

Author Contributions

L.Z. and C.R.P. contributed equally to this work. L.Z., C.R.P., H.B., and X.L. conceived the project and designed the experiments. L.Z., C.R.P., B.-A.J., H.B., and X.L wrote the manuscript. L.Z. and C.R.P. performed experiments and analyzed data. B.-A.J. and X.H. assisted with organoid preparation and cell culture. X.H. assisted with immunofluorescence staining. R.L. assisted with microscopy, and designed and 3D printed the supporting molds.

Keywords

bioengineering, collagen tube, droplet network, gastrointestinal tract, lipid bilayer

Received: September 2, 2020
Revised: October 23, 2020
Published online: November 25, 2020

[1] B. Greenwood-Van Meerveld, A. C. Johnson, D. Grundy, *Handb. Exp. Pharmacol.* **2017**, *239*, 1.
[2] R. H. Jones, *Aliment. Pharmacol. Ther.* **1996**, *10*, 233.
[3] H. Clevers, R. K. Conder, V. S. W. Li, M. P. Lutolf, L. Vallier, S. Chan, T. C. Grikscheit, K. B. Jensen, P. De Coppi, *Cell Stem Cell* **2019**, *24*, 855.
[4] J. Huang, Y. Ren, X. Wu, Z. Li, J. Ren, *J. Tissue Eng.* **2019**, *10*, 204173141983984.
[5] J. Costa, A. Ahluwalia, *Front. Bioeng. Biotechnol.* **2019**, *7*, 144.
[6] K. N. Bitar, E. Zakhem, *Nat. Rev. Gastroenterol. Hepatol.* **2016**, *13*, 543.
[7] E. Zakhem, S. Raghavan, R. R. Gilmont, K. N. Bitar, *Biomaterials* **2012**, *33*, 4810.
[8] Y. Chen, W. Zhou, T. Roh, M. K. Estes, D. L. Kaplan, *PLoS One* **2017**, *12*, e0187880.
[9] Y. Chen, Y. Lin, K. M. Davis, Q. Wang, J. Rnjak-Kovacina, C. Li, R. R. Isberg, C. A. Kumamoto, J. Mecsas, D. L. Kaplan, *Sci. Rep.* **2015**, *5*, 13708.
[10] T. C. Grikscheit, A. Siddique, E. R. Ochoa, A. Srinivasan, E. Alsberg, R. A. Hodin, J. P. Vacanti, *Ann. Surg.* **2004**, *240*, 748.
[11] T. Grikscheit, E. R. Ochoa, A. Srinivasan, H. Gaissert, J. P. Vacanti, *J. Thorac. Cardiovasc. Surg.* **2003**, *126*, 537.
[12] T. Grikscheit, A. Srinivasan, J. P. Vacanti, *J. Pediatr. Surg.* **2003**, *38*, 1305.
[13] K. Kitano, D. M. Schwartz, H. Zhou, S. E. Gilpin, G. R. Wojtkiewicz, X. Ren, C. A. Sommer, A. V. Capilla, D. J. Mathisen, A. M. Goldstein, G. Mostoslavsky, H. C. Ott, *Nat. Commun.* **2017**, *8*, 765.
[14] L. Urbani, C. Camilli, D. E. Phylactopoulos, C. Crowley, D. Natarajan, F. Scottoni, P. Maghsoudlou, C. J. McCann, A. F. Pellegata, A. Urciuolo, K. Deguchi, S. Khalaf, S. F. Aruta, M. C. Signorelli, D. Kiely, E. Hannon, M. Trevisan, R. R. Wong, M. O. Baradez, D. Moulding, A. Virasami, A. Gjinovci, S. Loukogeorgakis, S. Mantero, N. Thapar, N. Sebire, S. Eaton, M. Lowdell, G. Cossu, P. Bonfanti, P. De Coppi, *Nat. Commun.* **2018**, *9*, 4286.
[15] E. Hesse, T. E. Hefferan, J. E. Tarara, C. Haasper, R. Meller, C. Krettek, L. Lu, M. J. Yaszemski, *J. Biomed. Mater. Res. A* **2010**, *94*, 442.
[16] C. Bonnans, J. Chou, Z. Werb, *Nat. Rev. Mol. Cell Biol.* **2014**, *15*, 786.
[17] Y. Wang, D. B. Gunasekara, M. I. Reed, M. DiSalvo, S. J. Bultman, C. E. Sims, S. T. Magness, N. L. Allbritton, *Biomaterials* **2017**, *128*, 44.
[18] C. B. Weinberg, E. Bell, *Science* **1986**, *231*, 397.
[19] J. Hirai, K. Kanda, T. Oka, T. Matsuda, *ASAIO J.* **1994**, *40*, M383.
[20] N. Sachs, Y. Tsukamoto, P. Kujala, P. J. Peters, H. Clevers, *Development* **2017**, *144*, 1107.
[21] G. Villar, A. D. Graham, H. Bayley, *Science* **2013**, *340*, 48.
[22] L. Zhou, A. C. Wolfes, Y. Li, D. C. W. Chan, H. Ko, F. G. Szele, H. Bayley, *Adv. Mater.* **2020**, 2002183.
[23] H. Bayley, B. Cronin, A. Heron, M. A. Holden, W. L. Hwang, R. Syeda, J. Thompson, M. Wallace, *Mol. BioSyst.* **2008**, *4*, 1191.
[24] M. J. Booth, V. R. Schild, A. D. Graham, S. N. Olof, H. Bayley, *Sci. Adv.* **2016**, *2*, e1600056.
[25] A. D. Graham, S. N. Olof, M. J. Burke, J. P. K. Armstrong, E. A. Mikhailova, J. G. Nicholson, S. J. Box, F. G. Szele, A. W. Perriman, H. Bayley, *Sci. Rep.* **2017**, *7*, 7004.
[26] F. G. Downs, D. J. Lunn, M. J. Booth, J. B. Sauer, W. J. Ramsay, R. G. Klemperer, C. J. Hawker, H. Bayley, *Nat Chem* **2020**, *12*, 363.
[27] J. Drost, H. Clevers, *Development* **2017**, *144*, 968.
[28] J. K. Meier, M. Scharl, S. N. Miller, J. Brenmoehl, M. Hausmann, S. Kellermeier, J. Scholmerich, G. Rogler, *Inflammatory Bowel Dis.* **2011**, *17*, 202.
[29] A. Pastula, J. Marcinkiewicz, *Arch. Immunol. Ther. Exp.* **2019**, *67*, 19.
[30] M. Goke, M. Kanai, D. K. Podolsky, *Am. J. Physiol.* **1998**, *274*, G809.

© 2020 The Authors. Advanced Functional Materials published by Wiley-VCH GmbH

[31] Y. Nakase, T. Nakamura, S. Kin, S. Nakashima, T. Yoshikawa, Y. Kuriu, C. Sakakura, H. Yamagishi, J. Hamuro, Y. Ikada, E. Otsuji, A. Hagiwara, *J. Thorac. Cardiovasc. Surg.* **2008**, *136*, 850.
[32] K. Hayashi, N. Ando, S. Ozawa, Y. Kitagawa, H. Miki, M. Sato, M. Kitajima, *ASAIO J.* **2004**, *50*, 261.
[33] E. Bell, B. Ivarsson, C. Merrill, *Proc. Natl. Acad. Sci. USA* **1979**, *76*, 1274.
[34] B. Rothen-Rutishauser, A. Braun, M. Gunthert, H. Wunderli-Allenspach, *Pharm. Res.* **2000**, *17*, 460.
[35] I. Behrens, W. Kamm, A. H. Dantzig, T. Kissel, *J. Pharm. Sci.* **2004**, *93*, 1743.
[36] H. M. S. Algood, T. L. Cover, *Clin. Microbiol. Rev.* **2006**, *19*, 597.
[37] L. Buti, C. Ruiz-Puig, D. Sangberg, T. M. Leissing, R. C. Brewer, R. P. Owen, B. Sgromo, C. Royer, D. Ebner, X. Lu, *Proc. Natl. Acad. Sci. USA* **2020**, *117*, 2645.
[38] T. Sato, R. G. Vries, H. J. Snippert, M. van de Wetering, N. Barker, D. E. Stange, J. H. van Es, A. Abo, P. Kujala, P. J. Peters, H. Clevers, *Nature* **2009**, *459*, 262.
[39] K. P. O'Rourke, S. Ackerman, L. E. Dow, S. W. Lowe, *BioProtoc.* **2016**, *6*, 28.
[40] L. Buti, E. Spooner, A. G. Van der Veen, R. Rappuoli, A. Covacci, H. L. Ploegh, *Proc. Natl. Acad. Sci. USA* **2011**, *108*, 9238.

© 2020 The Authors. Advanced Functional Materials published by Wiley-VCH GmbH